Available online at www.sciencedirect.com
SCIENCE DIRECT®
Atmospheric Environment 40 (2006) 2911–2928
ATMOSPHERIC ENVIRONMENT
www.elsevier.com/locate/atmosenv

Scientific uncertainties in atmospheric mercury models I: Model science evaluation

Che-Jen Lin[a,*], Pruek Pongprueksa[a], Steve E. Lindberg[b,c,1], Simo O. Pehkonen[d], Daewon Byun[e], Carey Jang[f]

[a]*Department of Civil Engineering, Lamar University, Beaumont, TX 77710, USA*
[b]*Environmental Sciences Division, Oak Ridge National Laboratory, P.O. Box 2008, Oak Ridge, TN 37831–6038, USA*
[c]*Department of Natural Resources and Environmental Science, University of Nevada in Reno, Reno, Nevada 89557, USA*
[d]*Division of Environmental Science and Engineering, National University of Singapore, Singapore*
[e]*Department of Geosciences, the University of Houston, Houston, TX 77204, USA*
[f]*Office of Air Quality Planning & Standards, USEPA, Research Triangle Park, NC 27711, USA*

Received 20 October 2005; accepted 4 January 2006

Abstract

Eulerian-based, first-principle atmospheric mercury models are a useful tool to assess the transport and deposition of mercury. However, there exist uncertainty issues caused by model assumptions/simplifications and incomplete understanding of mercury science. In this paper, we evaluate the model science commonly implemented in atmospheric mercury models. The causes of the uncertainties are assessed in terms of gas phase chemistry, aqueous phase chemistry, aqueous phase speciation, aqueous phase sorption, dry deposition, wet deposition, initial and boundary conditions, emission inventory preparation, and domain grid resolution. We also present a new dry deposition scheme for estimating the deposition velocities of GEM and RGM based on RADM formulation. From our evaluation, mercury chemistry introduces the greatest uncertainty to models due to the inconsistent kinetic data and lack of deterministic product identification in the atmosphere. Model treatments of deposition velocities and aqueous Hg(II) sorption can also lead to distinct simulation results in mercury dry and wet depositions. Although model results may agree well with limited field data of GEM concentrations and Hg(II) wet deposition, it should be recognized that model uncertainties may compensate with each other to yield favorable model performance. Future research needs to reduce model uncertainties are projected.
© 2006 Elsevier Ltd. All rights reserved.

Keywords: Atmospheric mercury; Modeling; Chemical mechanism; Deposition; Mercury speciation; Aqueous sorption; Cloud water; Emission inventory; Initial and boundary conditions

1. Introduction

Mercury (Hg) is a persistent, bioaccumulative pollutant regulated by the United States Environmental Protection Agency (USEPA). The concern of mercury pollution arises from the health effects caused by methylated mercury ingestion through

*Corresponding author. Tel.: +1 409 880 8761; fax: +1 409 880 8121.
E-mail address: Jerry.Lin@lamar.edu (C.-J. Lin).
[1]Corporate Fellow Emeritus, now in Graeagle, CA 96103, USA.

1352-2310/$ - see front matter © 2006 Elsevier Ltd. All rights reserved.
doi:10.1016/j.atmosenv.2006.01.009

the consumption of fresh water and marine fish (Clarkson, 1995; USEPA, 1997). Mercury is released into the atmosphere from a variety of natural (Fitzgerald et al., 1998) and anthropogenic (Porcella et al., 1997) sources. It is recognized that anthropogenic emissions have greatly increased relative to natural sources since the onset of industrialization (Fitzgerald et al., 2005). Atmospheric mercury exists primarily as gaseous elemental mercury (GEM), reactive gaseous mercury (RGM, gaseous divalent mercury) and particulate mercury (PHg, mercury associated with atmospheric particles). GEM has a long atmospheric lifetime (0.5–2 yr), and can be transported over great distances. RGM and PHg have a much shorter lifetime and deposit back to the earth rapidly via dry and wet depositions (Schroeder and Munthe, 1998; Lin and Pehkonen, 1999; Keeler et al., 2005). Recently, the rapid deposition of gaseous mercury during the Polar sunrise raises concerns of mercury contamination in the Arctic and Antarctic Regions (Schroeder et al., 1998; Ebinghaus et al., 2002; Lindberg et al., 2002a). The background total mercury concentrations are 1–3 ng m^{-3} (Slemr et al., 2003).

Numerous modeling studies have been conducted to understand the fate of mercury in the atmosphere (e.g., Pai et al., 1997; Lin and Pehkonen, 1998b; Shia et al., 1999; Ryaboshapko et al., 2002, 2005; Bullock and Brehme, 2002; Seigneur et al., 2003, 2004). The simulation of atmospheric mercury is a challenging task, because it requires extensive treatment of multiple mercury species that exhibit distinct physical and chemical properties, and exist in multiple phases of the atmosphere. In addition, it has been demonstrated that atmospheric conditions and the presence of other pollutants can strongly affect the redox cycling of mercury (Lin and Pehkonen, 1998b). The diverse interactions between various mercury species and the atmospheric environment are complex and usually generate non-linear responses. Therefore, atmospheric mercury modeling requires careful consideration of emission, transport, chemical reactions, interfacial transfer/equilibria, cloud processes, and dry/wet depositions.

One difficulty in interpreting mercury modeling results is the uncertainty associated with the implemented model science. This is mainly caused by the different science parameterizations and the assumptions/simplifications made in the models. The uncertainties can come from multiple model components, including the preparation of emission inventories and speciation, the treatment of natural emission or so-called "re-emission" (Seigneur et al., 2004; Walcek et al., 2003; Lin et al., 2005), the chemical mechanisms in both gaseous and aqueous phases (Ryaboshapko et al., 2002), the uncertainty in the chemical kinetic constants (Van Loon et al., 2000; Gardfeldt and Jonsson, 2003; Pal and Ariya, 2004a, b; Calvert and Lindberg, 2005); the speciation of GEM oxidation products (Lin et al., 2004), and the treatment of mercury deposition schemes. These uncertainty issues require a thorough evaluation for the model improvement and future scientific implementation.

The objective of this paper is to assess the uncertainties resulting from the science components implemented in atmospheric mercury models. Earlier studies by Seigneur and coworkers have addressed the uncertainty issues in mercury emission and speciation, spatial resolution of model grids, treatment of mercury re-emission, effect of dry deposition velocity, boundary conditions, and precipitation fields (Pai et al., 1999, 2000; Seigneur et al., 2001, 2003a, 2004; Shia et al., 1999). In this effort, we will focus particularly on the uncertainty issues on chemical mechanisms, aqueous sorption, treatment of mercury dry deposition, and natural emissions. The results are presented in two companion papers. In the first paper, we evaluate the mercury science commonly implemented in first-principle, Eulerian-based atmospheric models, and present a new treatment of mercury dry deposition based on the RADM scheme. The causes for model uncertainties are discussed, and recommendations for model improvement are made based on current "state-of-the-science" of mercury. In Part II, we perform a series of sensitivity simulations to quantitatively assess the uncertainties using a modified version of CMAQ-Hg in a 36-km Continental Unites States domain.

2. Mercury model science evaluation and causes for uncertainties

2.1. Gas phase redox chemistry

The speciation, property, behavior and chemistry of atmospheric mercury chemistry have been reviewed by Lindqvist and Rodhe (1985), Schroeder et al. (1991), Schroeder and Munthe (1998), and Lin and Pehkonen (1999). Since then, a number of laboratory and theoretical studies have advanced the understanding on the transformation of mercury

in the atmosphere. The gaseous redox chemistry is dominated by the oxidation of GEM. The oxidants responsible for the oxidization include ozone (O_3, P'yankov, 1949; Hall, 1995; Pal and Ariya, 2004a), hydroxyl radical (OH, Sommar et al., 2001; Bauer et al., 2003; Pal and Ariya, 2004b), hydrogen peroxide (H_2O_2, Tokos et al., 1998), reactive halogens such as Cl, Cl_2, Br, Br_2, BrO, I, I_2 (Ariya et al., 2002; Calvert and Lindberg, 2003, 2004; Raofie and Ariya, 2003; Donohoue et al., 2005). Table 1 shows the reactions and their kinetic constants (Reactions G1–G8). Although there are other gaseous oxidants that may be responsible for GEM oxidation (e.g., NO_3, HO_2, O^{1D}, O^{3P}, HOCl, HOBr, etc. Schroeder et al., 1991; Lin and Pehkonen, 1999), the kinetic and mechanistic data are not available for model implementation and therefore are not discussed here.

The oxidation of GEM is the most dominant driving force for mercury deposition due to the much greater deposition velocity and water solubility of oxidized mercury compared to elemental mercury. Lin et al. (2004) compared the oxidation rate of GEM mediated by Reactions G1–G8 using the typical ambient concentrations of the oxidants in urban, rural airsheds and the marine boundary layer. They concluded that OH and O_3 dominate the GEM oxidation in the continental troposphere, while Cl and Br are the dominant oxidants in the marine boundary layer and the upper troposphere. Both OH and O_3 are photochemical oxidants, therefore it is expected that photochemical activities will facilitate mercury deposition. This indicates that urban air photochemical smog can enhance mercury deposition flux. Most chemical transport models (e.g., CMAQ, CAMx, REMSAD, etc.) have chemistry modules that estimate the concentration fields of OH and O_3 relatively well for calculating GEM oxidation. However, GEM oxidation by reactive halogens has not been treated extensively in atmospheric mercury models, although the activation and generation of reactive halogens and their chemical interactions with GEM have been investigated by various chemistry models (Calvert and Lindberg, 2003, 2004; Hedgecock and Pirrone, 2004; Hedgecock et al., 2003).

The uncertainties in the gaseous redox chemistry arise from two areas: (1) the uncertainty associated

Table 1
Current understanding of mercury reactions and kinetic parameters

No.	Mechanism	Rate constant	Type	Ref
Gas phase reactions				
G1	$Hg^0_{(g)} + O_{3(g)} \rightarrow HgO_{(s,\ g)} + O_{2(g)}$	$3\text{–}490 \times 10^{-20}\ cm^3\ molec^{-1}\ s^{-1}$	Ox	1–4
G2	$Hg^0_{(g)} + {}^{\bullet}OH_{(g)} \rightarrow Hg(II)$ Products	$8.7\text{–}9.0 \times 10^{-14}\ cm^3\ molec^{-1}\ s^{-1}$	Ox	5–7
G3	$Hg^0_{(g)} + H_2O_{2(g)} \rightarrow Hg(II)$ Products	$8.9 \times 10^{-19}\ cm^3\ molec^{-1}\ s^{-1}$	Ox	8
G4	$Hg^0_{(g)} + Cl_{2(g)} \rightarrow Hg(II)$ Products	$2.6 \times 10^{-18}\ cm^3\ molec^{-1}\ s^{-1}$	Ox	9
G5	$Hg^0_{(g)} + Br_{2(g)} \rightarrow Hg(II)$ Products	$< 9 \times 10^{-17}\ cm^3\ molec^{-1}\ s^{-1}$	Ox	9
G6	$Hg^0_{(g)} + Cl_{(g)} \rightarrow Hg(II)$ Products	$7.6\text{–}100 \times 10^{-13}\ cm^3\ molec^{-1}\ s^{-1}$	Ox	9,20
G7	$Hg^0_{(g)} + Br_{(g)} \rightarrow Hg(II)$ Products	$3.2 \times 10^{-12}\ cm^3 molec^{-1} s^{-1}$	Ox	9
G8	$Hg^0_{(g)} + BrO_{(g)} \rightarrow Hg(II)$ Products	$10^{-13}\text{–}10^{-15}\ cm^3\ molec^{-1}\ s^{-1}$	Ox	10
Aqueous phase reactions				
A1	$HgSO_{3(aq)} \rightarrow Hg^0_{(aq)} + S(VI)$	$T \exp(31.971T\text{–}12595)/T\ s^{-1}$	Red	11
A2	$Hg(SO_3)^{2-}_{2(aq)} \rightarrow Hg^0_{(aq)} + S(VI)$	$\ll 10^{-4}\ s^{-1}$	Red	12
A3	$Hg(OH)_{2(aq)} + UV \rightarrow Hg^0_{(aq)} + Products$	$3 \times 10^{-7}\ s^{-1}$, midday 60°N	Red	13
A4	$Hg(II)_{(aq)} + HO^{\bullet}_{2(aq)} \rightarrow Hg^0_{(aq)} + Products$	$1.7 \times 10^4\ M^{-1}\ s^{-1}$	Red	14
A5	$Hg^0_{(aq)} + O_{3(aq)} \rightarrow Hg^{2+}_{(aq)} + Products$	$4.7 \times 10^7\ M^{-1}\ s^{-1}$	Ox	15
A6	$Hg^0_{(aq)} + {}^{\bullet}OH_{(aq)} \rightarrow Hg^{2+}_{(aq)} + Products$	$2.0 \times 10^9\ M^{-1}\ s^{-1}$	Ox	16,17
A7	$Hg^0_{(aq)} + HOCl_{(aq)} \rightarrow Hg^{2+}_{(aq)} + Cl^- + OH^-$	$2.09 \times 10^6\ M^{-1}\ s^{-1}$	Ox	18
A8	$Hg^0_{(aq)} + OCl^-_{(aq)} \rightarrow Hg^{2+}_{(aq)} + Cl^- + OH^-$	$1.99 \times 10^6\ M^{-1}\ s^{-1}$	Ox	18
A9	$Hg^0_{(aq)} + HOBr_{(aq)} \rightarrow Hg^{2+}_{(aq)} + Br^- + OH^-$	$0.279\ M^{-1}\ s^{-1}$	Ox	19
A10	$Hg^0_{(aq)} + OBr^-_{(aq)} \rightarrow Hg^{2+}_{(aq)} + Br^- + OH^-$	$0.273\ M^{-1}\ s^{-1}$	Ox	19
A11	$Hg^0_{(aq)} + Br_{2(aq)} \rightarrow Hg^{2+}_{(aq)} + 2Br^-$	$0.196\ M^{-1}\ s^{-1}$	Ox	19

Refs.: (1) Pal and Ariya, 2004a; (2) Hall, 1995; (3) Schroeder et al., 1991; (4) P'yankov, 1949; (5) Pal and Ariya, 2004b; (6) Bauer et al., 2003; (7) Sommar et al., 2001; (8) Tokos et al., 1998; (9) Ariya et al., 2002; (10) Raofie and Ariya, 2003; (11) Van Loon et al., 2000; (12) Munthe et al., 1991; (13) Xiao et al., 1994; (14) Pehkonen and Lin, 1998; (15) Munthe, 1992; (16) Lin and Pehkonen, 1997; (17) Gardfeldt et al., 2001; (18) Lin and Pehkonen, 1998a; (19) Wang and Pehkonen, 2004; (20) Donohoue et al., 2005.

with the reported kinetic constants, and (2) the uncertainty in the oxidation product distribution. The kinetic uncertainty is especially troublesome for GEM oxidation by O_3 (Table 1, G1), since a wide range of rate constants have been reported ($4.2–49 \times 10^{-19}$ cm^3 $molec^{-1}$ s^{-1} by Schroeder et al., 1991 using the data by P'yankov, 1949; 3.0×10^{-20} cm^3 $molec^{-1}$ s^{-1} by Hall, 1995; and 7.5×10^{-19} cm^3 $molec^{-1}$ s^{-1} by Pal and Ariya, 2004a). The two most recent kinetic measurements show a range over a factor of 25. If the upper kinetic limit is used, ozone is the most important oxidant in the continental troposphere. However, if the lower limit is used, hydroxyl radical dominates the GEM oxidation according to the relatively consistent kinetic data (Table 1, G2) reported by Sommar et al. (8.7×10^{-14} cm^3 $molec^{-1}$ s^{-1}, 2001) and Pal and Ariya (9.0×10^{-14} cm^3 $molec^{-1}$ s^{-1}, 2004b). However, the occurrence of the GEM–OH reaction in the atmosphere has been questioned, and an upper limit of the rate constant (1.2×10^{-13} cm^3 $molec^{-1}$ s^{-1}) obtained from using an alternative kinetic technique (laser-induced fluorescence spectroscopy) was reported (Bauer et al., 2003).

More recently, Calvert and Lindberg (2005) performed a kinetic re-evaluation of the two mechanisms by thermodynamic calculations and chemical modeling. They suggested that the oxidative removal of GEM by O_3 may be significantly smaller than the laboratory kinetic predictions due to the possible dissociation of HgO in the atmosphere. The reported rate constant for Hg^0–OH reaction may also be very much overestimated due to the presence of other reactive radicals and O_3 during the generation of OH under the experimental conditions. Furthermore, since the oxidation of GEM by OH may be greatly attenuated by HgOH decomposition (Goodsite et al., 2004), the oxidation removal in the real atmosphere is potentially unimportant (Calvert and Lindberg, 2005). These contradicting results complicate the model science implementation.

Moreover, the oxidation products of GEM have not been clearly defined, causing a large uncertainty in the model prediction of mercury deposition fluxes. Understanding the product distribution between gas and aerosol (i.e., RGM vs. PHg) is important, since the deposition velocity and the removal mechanism of the mercury species vary greatly. For example, the deposition velocity of RGM has been estimated as high as 7.6 $cm\,s^{-1}$ with dry deposition as the primary removal pathway (Poissant et al., 2004). Actual field measurements of RGM are few, but those reported range from 1 to 4 $cm\,s^{-1}$ (Lindberg and Stratton, 1998). On the other hand, mercury associated with fine particulate matter (i.e., PHg) has a much smaller deposition velocity (usually <0.1 $cm\,s^{-1}$; Xu and Carmichael, 1998) and mainly removed by cloud scavenging and wet deposition.

Mercury oxidation products have not been studied extensively in earlier kinetic studies (e.g., Hall, 1995; Tokos et al., 1998; Sommar et al., 2001). More recently, Ariya and coworkers investigated the oxidation products of GEM by O_3, OH and a number of reactive halogens in the gaseous and particulate phases, as well as on the reactor wall using MS, GC–MS, ICP–MS and CI–MS (Ariya et al., 2002; Pal and Ariya, 2003, 2004a, b). These studies reported that the major fraction of the oxidation products is on the reactor walls. This is due to the relatively high Hg concentrations employed in the experiments that led to wall effects. Mercury oxidation by O_3 produces less than 1% of airborne PHg with HgO on the reactor walls identified as the primary product (Pal and Ariya, 2004a). However, Calvert and Lindberg (2005) argued that the production of HgO is unlikely in the atmosphere and that the laboratory-observed HgO may be an artifact from the decomposition of HgO_3 intermediates on reactor walls. They further proposed that the HgO_3 can survive thermal and photochemical decomposition, and transforms into $Hg(OH)_2$ or HgX_2 ($X = Cl$, Br) after depositing onto moist aerosols (Calvert and Lindberg, 2005). The oxidation by atomic and molecular halogens produces less than 0.5% PHg and the oxidation by OH produces 6% PHg and 10% RGM as HgO, the rest being wall-sorbed species (Ariya et al., 2002; Pal and Ariya, 2004b). Results from field measurements are also controversial, both RGM and PHg have been suggested as the primary products of GEM oxidation (e.g., Lindberg et al., 2002a; Lu et al., 2003). Stable Hg(I) species in gas phase has also been reported in a laboratory study from the oxidation of GEM by BrO (Raofie and Ariya, 2004), although its presence in the atmosphere has been questioned (Lin and Pehkonen, 1999).

Oxidation of GEM is the first and most important step for Hg removal from the atmosphere. Clearly, more theoretical and experimental studies are required on the kinetic parameters and the reaction products of mercury oxidation for a better model implementation. It will be most helpful if

exact chemical composition of RGM or PHg can be determined, which requires major analytical breakthrough for measuring the ultra-trace mercury speciation. The speciation has strong implications for the dry deposition implementation, since the physical properties of oxidized mercury can greatly affect the dry deposition velocity. Based on the known vapor pressure of HgX_2 (e.g., 8.99×10^{-3} Pa for $HgCl_2$ at 20 °C, Schroeder and Munthe, 1998) and the laboratory product study (Ariya et al., 2002), it is reasonable to assume that the GEM oxidation products by reactive halogens remain in the gas phase long enough to be detected. The reported HgO vapor pressure has a wide range from 2.53×10^{-6} to 9.20×10^{-12} Pa (Taylor, 1913; Bailar, 1973; Schroeder and Munthe, 1998). This yields a saturated HgO level ranging from $0.7\,pg\,m^{-3}$ to $0.2\,\mu g\,m^{-3}$, suggesting that HgO may possibly exist as PHg as well. However, elevated gaseous HgO levels have been detected in the laboratory from Hg^0 oxidation by OH and possibly by O_3 (Pal and Ariya, 2004a, b; Calvert and Lindberg, 2005). More studies are clearly needed to address these uncertainties in the oxidation product distribution.

2.2. Aqueous phase redox chemistry

Table 1 also shows the identified aqueous phase redox mechanisms of mercury (Reactions A1–A11). The identified aqueous oxidants are ozone (Munthe, 1992), hydroxyl radical (Lin and Pehkonen, 1997; Gardfeldt et al., 2001), $HOCl/OCl^-$ (Lin and Pehkonen, 1998a), and $Br_2/HOBr/OBr^-$ (Wang and Pehkonen, 2004). The reduction of aqueous Hg(II) is species specific (i.e., different Hg(II) complexes exhibit distinct kinetics), which is mediated by dissolved S(IV) (Munthe et al., 1991; Van Loon et al., 2000), HO_2 (Pehkonen and Lin, 1998) and via the photolysis of $Hg(OH)_2$. The concentration distribution of various Hg(II) complexes can be estimated from aqueous mercury speciation calculations (vide infra). The pH dependence of the oxidation by O_3 and OH and the reduction by HO_2 was not reported in the earlier kinetic studies.

The major uncertainties in the aqueous redox chemistry are from the reduction by HO_2 and S(IV). Pehkonen and Lin (1998) proposed a two-step reduction of Hg(II) by $HO_2^{\bullet}$ as an important reducing pathway based on a laboratory kinetic study. However, Gardfeldt and Jonsson (2003) argued that the aqueous Hg(II) reduction by $HO_2^{\bullet}/O_2^{\bullet-}$ should not occur under ambient conditions due to the possible re-oxidation of Hg(I) by dissolved oxygen before the second electron transfer can take place. A direct kinetic analysis of the Hg(II)–$HO_2^{\bullet}$ reaction is difficult (and not available in the literature), because the generation of the radical may also produce other oxidants and/or reductants that may interfere with the reaction itself. Since earlier model simulation indicates that $HO_2^{\bullet}$ may be the only significant aqueous reduction mechanism balancing Hg^0 oxidation after the depletion of aqueous S(IV) (Lin and Pehkonen, 1998b), further studies are needed to elucidate its kinetics and mechanism. The reduction of aqueous Hg(II) by S(IV) was first investigated by Munthe et al. (1991). A one-step, two-electron transfer with a first-order rate constant of $0.6\,s^{-1}$ was proposed for $HgSO_3$ complex at room temperature. Van Loon et al. (2000) re-evaluated the reduction kinetics and reported a much smaller rate constant ($0.0106\,s^{-1}$) with a temperature dependence that is generally accepted in the modeling community. The reduction by the photolysis of $Hg(OH)_2$ is not important based on the reported rate constant (Xiao et al., 1994; Lin and Pehkonen, 1998b).

2.3. Aqueous phase Hg(II) speciation

Aqueous speciation of divalent mercury [Hg(II)] has an important impact on the reaction kinetics. Hg(II) can form a wide variety of complexes with different aqueous ligands. This can be calculated by solving a series of parallel mass and charge balance equations using the expressions of equilibrium constants and the solution composition (Stumm and Morgan, 1995). Since Hg(II) has a very rapid water exchange rate in aqueous solutions (Brezonik, 1994), the formation of Hg(II) complexes does not limit the redox reaction rates, and can be treated separately as chemical equilibria. Table 2 shows the chemical equilibria and their stability constants relevant in atmospheric droplets. The organic ligands are neglected due to their much smaller concentration compared to the inorganic ligands. Hg(II) is a soft metal ion and it forms stable complexes with softer ligands such as Br^- and SO_3^{2-}, as indicated by the large stability constants in Table 2.

The total concentration of ligands and pH in atmospheric droplets are the most important factors affecting Hg(II) speciation. Lin and Pehkonen (1997, 1998b) calculated the aqueous speciation of

Hg(II) using the stability constants listed in Table 2. Based on the above studies and additional speciation calculations performed in this work, we summarize the speciation of Hg(II) in atmospheric droplets. Under a typical chemical composition in atmospheric droplets (Table 3), Hg(II) concentration is much lower than the ligand concentrations. The most important ligands that form significant complexes with Hg(II) are chloride (Cl^-) and sulfite [S(IV)], both as bis-complexes. Since aqueous sulfite comes from the dissolution of gaseous sulfur dioxide, the gaseous SO_2 concentration strongly affects the speciation of aqueous Hg(II). Furthermore, aqueous sulfite undergoes acid–base reactions (E1 and E2 in Table 2), therefore pH also affects the complex formation between Hg(II) and S(IV). At low S(IV) concentrations (i.e., $<0.1\,\mu M$), the dominant complex is $HgCl_2$. At higher S(IV) concentrations (i.e., $>1.0\,\mu M$), the most dominant Hg(II)–S(IV) complex is the relatively non-reactive $Hg(SO_3)_2^{2-}$ (Table 1, A2). Although the reactive $HgSO_3$ is not the dominating species under the typical conditions, its concentration peaks at about pH 4–5 (Lin and Pehkonen, 1998b) with a total aqueous sulfite concentration of about $1\,\mu M$. Under such conditions, S(IV) dominates the reduction of Hg(II).

Table 2
Chemical equilibria for calculating aqueous phase Hg(II) speciation

No.	Equilibrium	Log(K_{eq})
E1	$H_2O \cdot SO_2 \leftrightarrow H^+ + HSO_3^-$	−1.91
E2	$HSO_3^- \leftrightarrow H^+ + SO_3^{2-}$	−7.18
E3	$H_2O \cdot CO_3 \leftrightarrow H^+ + HSO_3^-$	−6.35
E4	$HCO_3^- \leftrightarrow H^+ + CO_3^{2-}$	−10.33
E5	$Hg^{2+} + OH^- \leftrightarrow Hg(OH)^+$	10.63
E6	$Hg^{2+} + 2OH^- \leftrightarrow Hg(OH)_2$	22.24
E7	$Hg^{2+} + SO_3^{2-} \leftrightarrow HgSO_3$	12.7
E8	$Hg^{2+} + 2\ SO_3^{2-} \leftrightarrow Hg(SO_3)_2^{2-}$	24.1
E9	$Hg^{2+} + OH^- + Cl^- \leftrightarrow HgOHCl$	18.25
E10	$Hg^{2+} + Cl^- \leftrightarrow HgCl^+$	7.30
E11	$Hg^{2+} + 2Cl^- \leftrightarrow HgCl_2$	14.0
E12	$Hg^{2+} + 3Cl^- \leftrightarrow HgCl_3^-$	15.0
E13	$Hg^{2+} + 4Cl^- \leftrightarrow HgCl_4^{2-}$	15.6
E14	$Hg^{2+} + Br^- \leftrightarrow HgBr^+$	9.07
E15	$Hg^{2+} + 2Br^- \leftrightarrow HgBr_2$	17.27
E16	$Hg^{2+} + 3Br^- \leftrightarrow HgBr_3^-$	19.7
E17	$Hg^{2+} + 4Br^- \leftrightarrow HgBr_4^{2-}$	21.2
E18	$Hg^{2+} + OH^- + Br^- \leftrightarrow HgOHBr$	19.7
E19	$Hg^{2+} + CO_3^{2-} \leftrightarrow HgCO_3$	11.0
E20	$Hg^{2+} + SO_4^{2-} \leftrightarrow HgSO_4$	1.34
E21	$Hg^{2+} + 2SO_4^{2-} \leftrightarrow Hg(SO_4)^{2-}$	2.40
E22	$Hg^{2+} + NO_3^- \leftrightarrow Hg(NO_3)^+$	0.11

Data are from Smith and Martell (2004).

At slightly to moderately acidic pH values in atmospheric droplets (pH 3–5.5), hydroxide (OH^-) and carbonate (CO_3^{2-}) ions are not at a sufficiently high concentration to form hydroxide and carbonate complexes with Hg(II). The contribution from bromide (Br^-) complexes can be significant in the marine boundary layer or in Polar Regions but negligible in the continental troposphere. With the very small stability constants between Hg(II) and sulfate (SO_4^{2-}) as well as nitrate (NO_3^-) ions, their complex formation is negligible. Since the lifetime of aqueous S(IV) is only a few hours (Lin and Pehkonen, 1998b), chloride is the most important ligand and it is a reasonable assumption that aqueous Hg(II) exist primary as $HgCl_2$. And the gas–liquid equilibrium of Hg(II) can be considered as the Henry's equilibrium of $HgCl_2$.

2.4. Aqueous phase sorption

Aqueous mercury can be adsorbed onto the solid phase in atmospheric droplets. The aqueous particulate matter can come from the insoluble fraction of cloud condensation nuclei (CCN) or the scavenging of PM from the gas phase. The aqueous-solid

Table 3
Typical concentrations of important atmospheric ions in droplets

Ions	Typical conc. (μM)	References/comments
Hg^{2+}	10^{-3}–10^{-5}	From data archived in mercury deposition network (MDN)
$[S(IV)]_{total}$	0–100	1–3
SO_4^{2-}	60–1500	1–3
NO_3^-	80–3000	1–3
Cl^-	10–2500	1–3
OH^-	10^{-5}–$10^{-2.5}$	Calculated from a typical droplet pH 3–5.5
$[Carbonate]_{total}$	$10^{-4.9}$	Calculated using effective Henry's constant at 351 ppmv CO_2 for pH 3–5.5

Refs.: (1) Erel et al., 1993; (2) Schell et al., 1997; (3) Seinfeld and Pandis, 1997.

equilibria are governed by sorption isotherms. However, quantitative assessment of the sorption of aqueous Hg(II) is difficult due to the uncertain nature of atmospheric particles in the aqueous phase (e.g., the identity of the particulate and the variability in its concentration). Earlier studies have suggested that a significant fraction of aqueous Hg(II) can be adsorbed onto the insoluble solids (e.g., Petersen et al., 1995; Seigneur et al., 1998). Seigneur et al. (1998) studied aqueous mercury sorption onto soot particles and atmospheric PM. They reported that 2–35% of aqueous Hg(II) is sorbed to the solid phase under their experimental conditions, and suggested that sorption kinetics should be considered. Aqueous sorption of Hg(II) can have an impact on the partitioning of mercury between the gas phase and atmospheric droplets. The adsorbed Hg(II) is considered removed from the aqueous phase and does not participate in the aqueous redox reactions. This inhibits the aqueous reduction of Hg(II), thus reducing the release of Hg^0 back to the gas phase (Lin and Pehkonen, 1998b) and enhancing RGM scavenging.

The aqueous sorption of metallic ions onto multiple sorbents (such as atmospheric PM) is a complex process and depends strongly on the solution composition and sorbent properties (Stumn and Morgan, 1996). As a simplification, aqueous Hg(II) adsorption is usually treated as simple sorption equilibrium (Pai et al., 1999; Seigneur et al., 1999) or a kinetic process estimated from sorption constants (e.g., Bullock and Brehme, 2002). With the low concentration of dissolved Hg(II) in atmospheric water, it is reasonable to use a simple linear sorption isotherm (Lin et al., 2004), and the total Hg(II) concentration in the aqueous phase can be expressed as

$$[Hg^{2+}]_{aq,total} = (1 + K_{ads}[APM]_{aq})[Hg_D^{2+}]_{aq}, \quad (1)$$

where $[Hg^{2+}]_{aq,total}$ is the total aqueous Hg(II) concentration in the dissolved and sorbed phases; K_{ads} is the soption constant; $[APM]_{aq}$ is the aqueous concentration of atmospheric particles; and $[Hg_D^{2+}]_{aq}$ is the dissolved Hg(II). However, there exists limited data describing the sorption characteristics of Hg(II) in the aqueous phase. Table 4 shows the sorption isotherms and the associated isotherm constants reported in recent Hg(II) adsorption studies. The sorption constants K_{ads} (as shown in Eq. (1)), is also estimated from the reported sorption parameters. The wide range in the values of K_{ads} poses a significant uncertainty in model implementation. For example, assuming a $10\,ng\,l^{-1}$ Hg(II) and $1\,mg\,l^{-1}$ of insoluble particulate matter in the aqueous phase, the ratio of sorbed Hg(II) to dissolved Hg(II) can range from 2.1×10^{-4} to 1.22 based on the range of the reported sorption constants.

2.5. Dry deposition

Mercury is removed from the atmosphere through both dry and wet depositions. Both removal pathways can cause contamination of mercury and their deposition contribution is comparable. The dry deposition of mercury exhibits a strong seasonal variation, with enhanced deposition fluxes during the summer months (Lindberg et al., 1992; Vanarsdale et al., 2005). The deposition flux is estimated by the product of the deposition velocity and gaseous concentration for various mercury species, i.e.,

$$F_{dry} = V_d \times C_g, \quad (2)$$

where F_{dry} is the dry deposition flux ($ng\,m^{-2}\,h^{-1}$), V_d is the dry deposition velocity ($m\,s^{-1}$) and C_g is the gaseous concentration of mercury species (i.e., GEM, RGM or PHg) in $ng\,m^{-3}$. Experimentally, V_d can be estimated by mercury flux measurements by micro-meteorological techniques (Xu et al., 1999; Lindberg et al., 1998, 2002b). The measured deposition velocity shows a diurnal pattern, with peak values during midday. The reported daytime dry deposition velocities of GEM, PHg and RGM can reach 0.19, 2.1 and $7.6\,cm\,s^{-1}$, respectively (Poissant et al., 2004), with much lower values at night due to reduced atmospheric turbulence (Lindberg et al., 1992). Although the dry deposition velocity of GEM is much smaller compared to PHg and RGM, its deposition may still be important due to the much greater concentration of GEM compared to those of RGM and PHg (Lee et al., 2001).

The model treatment of mercury dry deposition velocity varies greatly in atmospheric mercury models. The dry deposition velocity of GEM is often neglected (e.g., Bergan and Rodhe, 2001; Bullock, 2000; Bullock and Brehme, 2002), assigned a very small value (e.g., $0.015\,cm\,s^{-1}$, Lee et al., 2001), or treated as surface uptakes (Xu et al., 2000; Lin and Tao, 2003). The dry deposition of fine particulate matter (e.g., the accumulation mode size regime) is usually used as a surrogate V_d for PHg (e.g., Bullock and Brehme, 2002; Pai et al., 1999). The deposition velocity of RGM is either assumed

Table 4
Sorption isotherms and the associated constants for aqueous phase Hg(II) adsoprtion

Sources	Xiao and Thomas (2004)	Budinova et al. (2003)	Sanchez-Polo and Rivera-Utrilla (2002)	Manohar et al. (2002)	Karabulut et al. (2001)	Seigneur et al. (1998)	Yin et al. (1997)
Sorbents	Activated carbon, 0.002 g mL^{-1}	Furfural-based carbon, 0.0002 g mL^{-1}	Ozonated activated carbon, Φ = 500–800 μm, pH_{pzc}: 2.6–8.8, 0.002 g mL^{-1}	Clay (Φ = 0.096 mm, As = 71.3 m^2 g^{-1}, porosity = 0.39 ml g^{-1}, ρ = 1.39 g mL^{-1}, cation exchange capacity: 2.3 meq g^{-1}, pH_{pzc}: 3.4, 0.002 g mL^{-1}	Coal (lignite), 65 mesh ASTM, 1 g mL^{-1}	Atmospheric particulate matter, Φ < 62 μm, 20 mg L^{-1}	15 Soil types (sand-loam), Φ < 2 mm, 0.01 g mL^{-1}
Hg conc.	$Hg(NO_3)_2$: 48–4173 μM	$HgCl_2$: 10–40 mg L^{-1}	50 mg L^{-1} Hg(II)	25–1000 mg L^{-1} Hg(II)	10–100 ppm Hg(II)	THg: 1.67 ng L^{-1}	$Hg(NO_3)_2$: 1.0×10^{-7}–1.1×10^{-4} M
Solution conditions	T: 25 °C, pH: 1.97–3.90	pH: 2.0–5.0	T: 25 °C, pH: 2.0–12.0	T: 30–60 °C, pH: 4.0–8.0	T = 25 ± 2 °C, pH: 2.0–6.0	pH: 3.1–6.1	T = 25 ± 2 °C, pH = 4.9–6.5. I = 0.001–0.1 M $NaNO_3$
Sorption model[a]	q_{max}: 1.06–1.37 mmol g^{-1}, K_{ads}: 1.82–7.87 L mmol^{-1}	q_{max}: 134–174 mg g^{-1}, K_{ads}^{-1}: 0.11–1.40 mg L^{-1}	q_{max}: 38.61–62.11 mg g^{-1}, K_{ads}: 0.06–0.57 L mg^{-1}	q_{max}: 46.02–70.32 mg g^{-1}, K_{ads}: 0.037–0.1231 mg^{-1}	q_{max}: 2.03 mg g^{-1}, K_{ads}^{-1}: 9.81 mg L^{-1}	—	Log K_{ads}: 5.16–5.97 L mol^{-1}, q_{max}: 3.73–12.80 μmol g^{-1}
K_{ads}, L g^{-1}[b]	1.93–10.78	124–1218	2–11	1.7–8.6	0.21	3–91	0.54–10.26

[a]All the sorption models are based on Langmuir isotherm except Seigneur et al. (1998).
[b]The K_{ads} (as shown in Eq. (1)) values are calculated from the linear range of the Langmuir isotherm using the sorption parameters reported in the sorption models.

(0.5–4.0 cm s^{-1}, Bergan and Rodhe, 2001; Hedgecock and Pirrone, 2004; Lee et al., 2001), assigned as the deposition velocity of HNO_3 as a surrogate V_d (Bullock and Brehme, 2002; Xu et al., 2000), or treated using resistance modeling approaches (Lindberg et al., 1992; Pai et al., 1997, 1999). The wide range of treatments in the dry deposition scheme introduces a large uncertainty in model estimates of deposition flux.

Treating the dry deposition of various mercury species using the resistance analog has several advantages compared to the assigned deposition velocities, since resistance models consider the effect of different land uses, and they are capable of characterizing the diurnal variation of dry deposition velocities. The resistance model is expressed as

$$V_d = (R_a + R_b + R_c)^{-1} + V_g, \quad (3)$$

where R_a (s m^{-1}) is the aerodynamic resistance estimated from turbulent transport; R_b (s m^{-1}) is the quasi-laminar resistance estimated from mercury diffusivities; R_c (s m^{-1}) is the canopy/surface resistance; V_g (m s^{-1}) is the settling velocity in the case of coarse particulate matter (PHg, $>2.5\,\mu m$). For mercury, the dominant term in Eq. (3) is the canopy/surface resistance. Using the published deposition models for canopy resistance (Baldocchi, 1988; Du and Fang, 1982; Hicks and Meyers, 1988), Lindberg et al. (1992) showed the diurnal variation of GEM dry deposition velocity. The mean daytime V_d to a deciduous forest was estimated to be 0.12 and 0.006 cm s^{-1} in summer and winter, respectively. Lindberg et al. (2002b) first reported a measured V_d of 0.14 ± 0.13 cm s^{-1} under a similar meteorological condition for GEM to cattail canopy. Pai et al. (1999) used the canopy resistance of SO_2 for estimating Hg^0 dry deposition velocity, since mercury diffusivity is close to that of SO_2 (Lindberg et al., 1992).

Rigorous treatment of deposition velocity of GEM, RGM and PHg is possible with knowledge of mercury thermodynamic/physical properties. Using the formulation of RADM deposition scheme (Wesely, 1989), we estimated the canopy resistance of GEM and RGM:

$$R_c = \left(\frac{1}{r_{sx} + r_{mx}} + \frac{1}{r_{lux}} + \frac{1}{r_{dc} + r_{clx}} + \frac{1}{r_{ac} + r_{gsx}} \right)^{-1}. \quad (4)$$

The definition of the resistance terms in Eq. (4) and their calculations are shown in Table 5. Eq. (4) and Table 5 consider the effect of atmospheric stability and different land use types based on the 3-D wind fields and GIS information. It also incorporates the physical properties (e.g., Henry's Law constants and diffusivities) of various mercury species in the V_d estimate. Finally, it generates a diurnal pattern similar to the observed deposition velocities of trace gases.

Using Eq. (4) and assuming RGM species as $HgCl_2$ or HgO (since the product speciation has yet to be determined), we estimated the magnitude and diurnal patterns of the deposition velocities of GEM and RGM in summer and winter. Fig. 1 shows the simulated monthly average deposition velocity of GEM (Fig. 1a and b) and RGM (Fig. 1c and d as $HgCl_2$ and Fig. 1e and f as HgO) in typical winter (Fig. 1a, c and e) and summer conditions (Fig. 1b, d, and f) in a 36-km continental US domain (the model setup is shown in the figure caption). Clearly, the summertime (i.e., July) deposition velocity is greater compared to the wintertime (i.e., December) due to the much lower aerodynamic resistance. In our calculation, the hourly average peak V_d values for GEM, $HgCl_2$ and HgO are 0.09, 3.44 and 6.86 cm s^{-1} in July, and 0.07, 3.10 and 6.64 cm s^{-1} in December, respectively. In Fig. 1, the elevated V_d values above part of the sea surface area in January (Fig. 1a, c and f) is caused by the lower aerodynamic resistance calculated from the meteorological data. Generally, the greatest deposition velocities are observed with the land use type of coniferous forest, because of its greater leaf surface area on a year-round basis.

Fig. 2 shows the average diurnal variations of mercury deposition velocities in the entire model domain. It can be observed that assuming RGM as $HgCl_2$ versus HgO has a strong impact on the calculated dry deposition velocities, mainly caused by the difference in their respective Henry's Law constants (Table 5). According to Calvert and Lindberg (2005), $HgCl_2$ is more likely to have a significant lifetime in the gas phase. Gaseous HgO, if formed, will probably tend to attach to the aerosol phase. Nevertheless, the difference on the calculated V_d values will lead to a large difference in the RGM deposition flux from model estimates. Deterministic identification of RGM species will thus reduce the uncertainty in the dry deposition analysis. In addition, more field data are needed to verify the species-specific deposition velocities.

Table 5
RADM parameters used for estimating the canopy resistance of GEM and RGM[a]

Terms	Formulation	Description	Remarks	
r_{dc}	$100[1+1000(G+10)^{-1}]$ $(1+1000\,q)^{-1}$	Buoyant convection resistance		
r_{sx}	$r_s D_{H_2O}/D_x$, where $r_s = r_i$ $\{1+[200(G+0.1)]^{-1}]^2\}$ $\{400[T_s(40-T_s)]^{-1}\}$	Stomatal resistance for substance x	HNO_3	$D_{H_2O}/D_{HNO_3} = 1.9$
			RGM	$D_{RGM} = 0.086\,cm^2\,s^{-1}$; $D_{H_2O}/D_{RGM} = 2.53$
			GEM	$D_{GEM} = 0.1194\,cm^2\,s^{-1}$; $D_{H_2O}/D_{RGM} = 1.82$
r_{clx}	$[k_H/(10^5 r_{cls}) + f_0/r_{clO}]^{-1}$	Lower canopy resistance	HNO_3	$K_H = 1\times10^{14}\,M\,atm^{-1}$; f_0 $(HNO_3) = 0.0$
r_{gsx}	$[k_H/10^5 r_{gsS}) + f_0/r_{gsO})]^{-1}$	Ground surf. resistance	RGM	$K_H = 2.8\times10^6\,M\,atm^{-1}$ ($HgCl_2$)
r_{mx}	$(k_H/3000 + 100\,f_0)^{-1}$	Mesophyll resistance		$K_H = 2.7\times10^{12}\,M\,atm^{-1}$ (HgO) f_0 (RGM) = **0.1 or 1.0**
r_{lux}	$r_{lu}\,(10^{-5}\,k_H + f_0)^{-1}$	Leaf cuticular resistance	GEM	$K_H = 0.139\,M\,atm^{-1}$ (GEM) f_0 (GEM) $= 10^{-5}$
	$[1/(3r_{lu}) + 10^{-7}\,k_H + f_0/r_{luO}]^{-1}$	Dew or rain correction		
r_{lus}	100	Leaf cuticular, SO_2 (dew)		
	$[1/5000 + 1/(3r_{lu})]^{-1}$	Rain correction		
r_{luO}	$[1/3000 + 1/(3r_{lu})]^{-1}$	Leaf cuticular, O_3 (dew)		
	$[1/1000 + 1/(3r_{lu})]^{-1}$	Rain correction		

[a] G is the solar radiation reaching the canopy, D_x is the molecular diffusivity of the trace species, r_i is the minimum bulk canopy stomatal resistance for water vapor, r_{lu} is the surface bulk resistance component for leaf cuticles in healthy vegetation and otherwise the outer surfaces in the upper canopy, r_{clS} is the surface bulk resistance component for leaves, twig, bark or other exposed surfaces in the lower canopy to SO_2, r_{clO} is the surface bulk resistance component for leaves, twig, bark or other exposed surfaces in the lower canopy to O_3, r_{ac} is the surface bulk resistance component for transfer that depends only on canopy height and density, r_{gsS} is the surface bulk resistance component for the soil, leaf litter, etc. at the ground surface to SO_2, r_{gsO} is the surface bulk resistance component for the soil, leaf litter, etc. at the ground surface to O_3. These parameters depend on land uses and seasons; f_0 is the reactivity constant as defined by Wesley (1989).

2.6. Wet deposition

Previous studies have shown that wet deposition is a major removal pathway for atmospheric mercury (Keeler et al., 2005; Miller et al., 2005). Wet deposition of mercury results from mercury oxidation followed by the scavenging of oxidized mercury into atmospheric droplets, and the removal by precipitation to the Earth's surface (i.e., rainout). These processes are controlled by the gaseous and aqueous mercury chemistry, the interfacial transfer of RGM and PHg and the sorption process in the aqueous phase. The wet deposition flux of mercury can be estimated according to

$$F_{wet} = P \times [Hg^{2+}]_{aq,total}, \quad (5)$$

where F_{wet} is the wet deposition flux ($ng\,m^{-2}\,h^{-1}$), P is the precipitation intensity ($m\,h^{-1}$) and $[Hg^{2+}]_{aq,total}$ is defined as in Eq. (1). Seigneur et al. (2001) also considered the below cloud scavenging (i.e., washout) in their wet deposition treatment. The major uncertainty here is from the inaccuracy of the precipitation fields and the assumptions made in the cloud scavenging process (Seigneur et al., 2001). Current model treatments assume that (1) all PHg is incorporated into the aqueous phase upon cloud formation, (2) the sorbed Hg(II) in the aqueous phase is considered as PHg, and (3) the scavenging of GEM and RGM is based on Henry's Law equilibrium (e.g., Bullock and Brehme, 2002). These assumptions on cloud processing are very simplified without robust treatment of cloud microphysics and release of PHg from clouds. Since cloud cover and precipitation from meteorological models can be very different from the ground and satellite observations (e.g., Biazar et al., 2005), and current model predictions of aqueous mercury concentration correlated reasonably well with field measurements (Lin and Pehkonen, 1998b; Seigneur et al., 2001, 2004), the uncertainty in the precipitation fields has the strongest impact on model prediction on wet mercury deposition. Therefore, careful inspection of the precipitation data in the

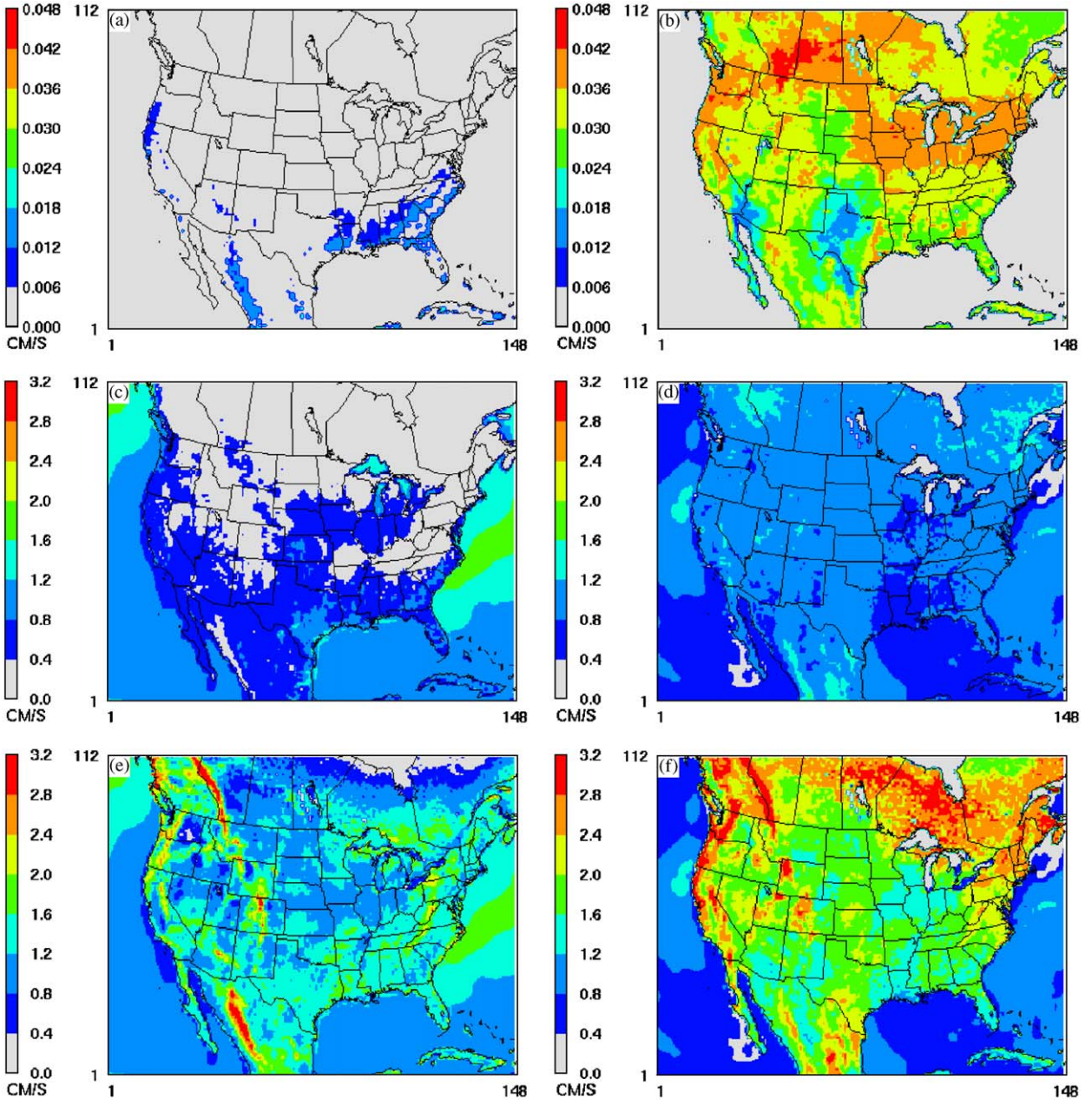

Fig. 1. The simulated monthly average deposition velocity of GEM and RGM. (a) GEM in January. (b) GEM in July. (c) RGM as $HgCl_2$ in January. (d) RGM as $HgCl_2$ in July. (e) RGM as HgO in January. (f) RGM as HgO in July. The calculation was performed in a 36-km US domain using the USEPA 2001 MM5 meteorology. The spatial feature of the average deposition velocity is caused by the different land uses and the meteorological data. Notice that the color scales for GEM and RGM are different. See text for discussion.

meteorological fields is needed for the interpretation of modeled mercury wet deposition results.

2.7. Emission inventory estimates and speciation

The mercury emission from anthropogenic sources is several orders of magnitude smaller than other regulated pollutants (e.g., SO_2, NO_x, CO, PM, etc). In our modeling analysis, we have observed that the total ambient gaseous concentration of mercury is not significantly modified from their background concentrations, except near major point sources. This agrees with previous modeling assessment (e.g., Seigneur et al., 2001, 2004). The

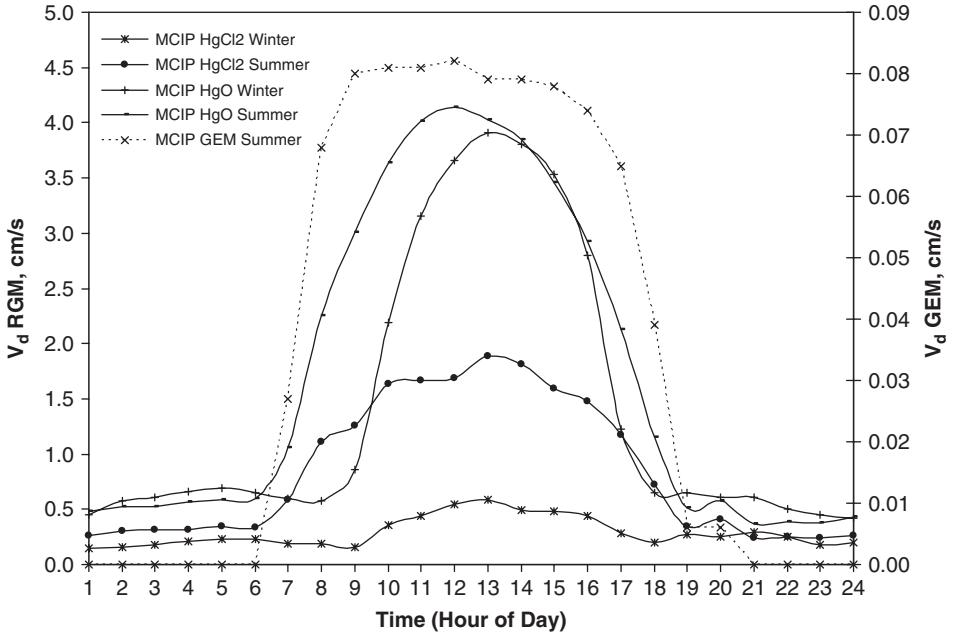

Fig. 2. The domain-average diurnal variation of mercury deposition velocities. The speciation of RGM as HgO and $HgCl_2$ can lead to distinct deposition velocities.

global anthropogenic emission inventory estimate of mercury is continuously being revised and improved (Pacyna et al., 2001, 2003; Hylander and Meili, 2003). Generally, the emission inventory estimate in North America is relatively reliable, mainly due to the integrated efforts of governmental programs and private industries in compiling and revising the USEPA National Emission Inventory (NEI) and the Toxic Release Inventory (TRI). There is an uncertainty factor of 3 for Hg emissions in Mexico and an uncertainty factor of approximately 2 in Europe (Seigneur et al., 2001). Recently, several emission inventory re-assessments and field campaigns have provided more reliable estimates of mercury emission in East Asia (Streets et al., 2005). Nevertheless, significant uncertainties (usually underestimates) still remain in these estimates due to the lack or inaccuracy in reported emission data, stack measurements of Hg, and capture of Hg in control devices.

The natural emission caused by previously deposited mercury is also highly uncertain, mainly due to the lack of a comprehensive, mechanistic description of the natural emission process (Lindberg et al., 2005). Recent isotopes studies suggested that an important fraction of mercury deposited to both terrestrial and aquatic surfaces are re-emitted (Lindberg et al., 2003). This so-called ''mercury re-emission'' is similar in magnitude to the anthropogenic mercury emission, especially in summer (Lindberg et al., 1998; Lin et al., 2005). The characteristic emission differences between the mercury re-emission from natural processes and anthropogenic emission are: (1) the re-emission exhibits strong diurnal and seasonal variations, while the variation of anthropogenic emissions is much smaller; (2) the natural processes emit mainly GEM, while anthropogenic emissions release GEM, RGM and PHg depending on the sources, fuel types and control devices employed; (3) the natural processes emit mercury to the surface layer of the model domain only, while anthropogenic emissions from point sources are subject to plume rise depending on atmospheric stability; and (4) the natural processes are relatively weaker and more diffused compared to anthropogenic emissions, but cover a much larger area.

The emission of mercury through natural processes has been overlooked or treated as a fraction of the deposited mercury in the preparation of gridded mercury emission inventory (e.g., Bergan and Rodhe, 2001; Bullock and Brehme, 2002). Lin and Tao (2003) and Xu et al. (2000) incorporated this emission contribution through bi-directional air-surface exchange of GEM vapor. Seigneur et al. (2004) estimated that the mercury ''re-emission to

deposition'' ratio ranges from a lower limit of 33% to an upper limit of 56%. More recently, emission processors extensively treating the emission from vegetation, water surface and soils have been developed based on a simplified mechanistic (Bash et al., 2004) or a regression (Lin et al., 2005) approach to assimilate the observed evasion fluxes of mercury. Such treatments provide highly temporally and spatially resolved natural mercury emissions. However, more field and mechanistic studies of the natural emission process are clear needed for better model parameterization.

The emission speciation of mercury has a profound impact on the modeled mercury deposition, especially near the emission sources. GEM is subject to long-range transport; while RGM (and PHg to a less extent) deposits rapidly near the emission sources. Since the natural emission speciation is dominated by GEM, the speciation assignment of anthropogenic emission of mercury has particularly strong implications for mercury dry and wet deposition on a regional scale. The speciation of mercury emission depends on the fuel types and the use of emission control technology (Senior et al., 2000; Senior and Johnson, 2005). Its characterization requires comprehensive in-stack measurements at the emission sources. In the United States, the compilation of NEI greatly reduces the uncertainty of mercury emission speciation, since the fuel types and control devices are well documented, although some uncertainty for area source emission still remains. In Asia, the speciation data are not readily available and cautions should be taken in interpreting model results of local deposition.

2.8. Initial and boundary conditions

Initial and boundary conditions (IC/BC) represent the starting mercury concentrations and out-of-boundary transport input into the model domain in the simulations. By default, it is more favorable to generate the IC/BC from a coarse domain using model nesting to provide a better spatial distribution of GEM, RGM and PHg. The IC/BC of GEM has an impact on the modeled deposition flux forced by chemical oxidation. The IC for RGM and PHg has no impact on mercury deposition after a short model spin-up, and the BC do not have a significant effect on model deposition away from the domain boundary due to the rapid RGM/PHg removal and scavenging. Pai et al. (1999) varied the RGM boundary conditions in a North American domain and observed that the impact of the BC change is negligible. In our modeling analysis, we have observed the BC of RGM and PHg can cause significantly higher dry and wet deposition near the domain boundary (up to 5–10 modeling grids in the 36-km domain). Therefore, caution should be taken in interpreting the modeled deposition results for small domains or the grids near the domain boundaries.

2.9. Domain grid resolution

The effect of domain grid resolution on the modeled mercury deposition is two-fold. First, since chemical transport models assume instantaneous mixing (thus diluted) of emitted pollutants in the receiving model grids, changes in the grid resolution directly influence the resulting dilution near the emission locations. Secondly, it results in a change in the GIS data resolution, which can affect the vertical mixing of pollutants. An increase in the domain grid size dilutes the concentration of various mercury species. For GEM, this dilution reduces the chemical oxidation rate and thus the deposition flux. For RGM and PHg, the dilution also decreases the tendency of dry deposition, since the deposition flux is proportional to the gaseous concentration (Eq. (2)). As the gaseous mercury concentration can be modified significantly near large emission sources, the effect of a grid resolution change is more important near the sources, due to both emission dilution and lower concentration of photochemical oxidants responsible for GEM oxidation. Pai et al. (2000) tested the effects of grid resolution on the dry and wet deposition of mercury by varying the grid size from 100 to 20 km in a regional northeast US domain. They reported that the short-term peak dry deposition flux can be increased by a factor of 2 in the 20-km domain. However, the difference in dry deposition in remote areas as well as in wet deposition of the entire domain is much smaller (Pai et al., 2000). For simulations in coarser grids, implementation of plume-in-grid should provide a more realistic mercury concentration field near the emission points for modeling local mercury deposition.

2.10. Other modeling issues

Recently, there has been substantial research devoted to the rapid dry deposition of oxidized mercury during the Polar sunrise, so called ''mer-

cury depletion events" or MDEs, (e.g., Schroeder and Munthe, 1998; Ebinghaus et al., 2002; Lindberg et al., 2002a; Skov et al., 2004), and to the much shorter atmospheric lifetime of mercury in the marine boundary layer (Hedgecock and Pirrone, 2004; Hedgecock et al., 2003; Laurier et al., 2003). Field and modeling studies have suggested that the enhanced mercury removal is mediated by the oxidation of GEM by a number of reactive halogen species (e.g., Br, Cl, Br_2, Cl_2, BrO, ClO and possibly others) followed by a rapid deposition of RGM and/or PHg (Calvert and Lindberg, 2003, 2004; Lu et al., 2003). It has been suggested that these oxidation pathways can strongly affect the global cycling budget of mercury (Mason and Sheu, 2002). There is also an increasing concern for the intercontinental transport of mercury and mercury deposition in coastal regions (Streets et al., 2005; Jaffe et al., 2005). However, current chemical transport models of mercury do not have the capability to simulate these processes. The model implementation of such processes requires extensive treatment and parameterization of sea salt aerosol generation and reactive halogen activation (Keene et al., 1993; Vogt et al., 1996; Spicer et al., 1998; Keene et al., 1999; Von Glasow et al., 2002a, b; Knipping and Dabdub, 2002), as well as reliable chemical mechanisms and kinetic data. More research is needed to elucidate the oxidation of GEM by reactive halogens to facilitate a more robust model implementation.

3. Implications for atmospheric mercury simulations

A number of atmospheric mercury models have a reasonably good capability in predicting long-term average GEM concentrations and total wet deposition of mercury (Pai et al., 1997, 1999; Seigneur et al., 2001, 2003b, c; Ryaboshapko et al., 2005 and the references cited therein). Interestingly, these models incorporate different parameterizations in the treatment of chemical mechanisms, wet and dry deposition schemes, and emission inventories with different model assumptions, thus having different areas of model uncertainties. With the complex physical and chemical processes that mercury undergoes in the atmosphere, the model uncertainties may compensate each other. Therefore, the model agreement with limited field measurements should not be considered as model accuracy. Caution should be exercised to understand the direction and magnitude of model biases caused by the model and/or scientific uncertainties in order to better interpret the simulation results.

One of the challenges in atmospheric mercury simulation is that there are still many atmospheric processes involving mercury that are not well understood, and sometimes contradictory scientific information exists in the literature. This complicates the science implementation, and some simplifications must be made to obtain the model results. The other challenge is that there is a general lack of continuous field and network measurement data of atmospheric mercury (e.g., concentration, speciation, and dry deposition) for a proper model calibration and verification. Most the modeling results compared favorably with long-term wet deposition data and total gaseous mercury concentrations, the later often dominated by background concentrations. The availability of additional field data for model verification will certainly help reduce model uncertainties. Finally, the currently measurable species of atmospheric mercury are loosely defined, except GEM. The exact chemical species of RGM, which plays an important role in the dry and wet deposition treatment of mercury, have not been analytically defined due to the analytical difficulty in determining ultra-trace air pollutants such as mercury. Without such chemical information, explicit treatment of mercury species in the model is difficult, if not impossible, and uncertainties remain. Also needed are better measurements of the particle size distribution of PHg to better assess its dry deposition. Current assignment of PHg into fine particulate mode results in negligible PHg deposition in the model (e.g., Bullock and Brehme, 2002).

One approach to address model uncertainty issues is to perform sensitivity analyses on various model components and parameters. This defines the upper and lower bounds of the model outcomes of the uncertainties. In the next companion paper, we perform sensitivity simulations to address the effects of varied chemical mechanisms, dry deposition schemes, aqueous sorption and the incorporation of natural emissions on modeled Hg deposition fluxes.

4. Conclusions

Of the greatest importance for reducing model uncertainties is the accurate quantification of the reaction kinetics of mercury transformation mechanisms in both gas and aqueous phases. The current understanding of atmospheric mercury

chemistry and related kinetics are based on the extrapolation of limited laboratory investigations. The appropriateness of such extrapolation has been questioned (e.g., Calvert and Lindberg, 2005; Gardfeldt and Jonsson, 2003). In addition, some of the reaction kinetics and products are not clearly defined. Since chemistry is the most important driving force for mercury deposition in regions away from the anthropogenic sources, further experimental investigations addressing these kinetic and product uncertainties will greatly improve model performance in predicting both dry and wet depositions.

Based on the published stability constants and water exchange rate constants, it is reasonable to assume that aqueous phase speciation will not kinetically limit the chemical reactions of mercury in droplets. The most dominant aqueous Hg(II) species is $HgCl_2$ under typical droplet conditions. There is a lack of knowledge in the interactions between mercury species and atmospheric particulates and more studies are needed. The aqueous adsorption equilibrium of Hg(II) onto insoluble particles should be better quantified to assess the contribution of sorbed Hg(II) in wet mercury deposition. Extensive treatment for estimating dry deposition velocity is possible with the published dry deposition schemes and the knowledge of thermodynamic properties of various mercury species, although field examination of the modeled dry deposition velocities is still much needed. Both IC/BC and grid resolution can affect the model results of mercury deposition. Due to the relatively small emission quantity of mercury into the atmosphere compared to other criterion pollutants, the modification of total gaseous mercury concentration by emissions is not significant, except near major emission sources. However, the assignment of mercury emission speciation has a profound impact on mercury deposition near the anthropogenic sources. Since models may incorporate different scientific parameterizations, it is important to recognize the direction and magnitude of model biases caused by the uncertainties to better interpret model simulation results.

Acknowledgments

The authors would like to acknowledge the funding support from Texas Commission on Environmental Quality (TCEQ Work Order No. 64582-04-10) and the USEPA (RTI Subcontract No. 3-92U-9606). Lin and Pongprueksa would like to thank the facility support from Dr. Thomas C. Ho, Dr. Hsing-wei Chu, Drs. Jack R. Hopper and Dr. Robert Yuan in the College of Engineering at Lamar University. We also thank Dr. Christian Seigneur and Russell Bullock for their insightful discussions. This study represents the scientific opinions of mercury modeling issues by the authors and does not reflect the views of the funding agencies.

References

Ariya, P.A., Khalizov, A., Gidas, A., 2002. Reactions of gaseous mercury with atomic and molecular halogens: kinetics, product studies, and atmospheric implications. Journal of Physical Chemistry A 106, 7310–7320.

Bailar, J.C., 1973. Comprehensive Inorganic Chemistry. Pergamon Press, New York.

Baldocchi, D.D., 1988. A multilayer model for estimating sulfur dioxide deposition to a deciduous oak forest canopy. Atmospheric Environment 22, 869–884.

Bash, J.O., Miller, D.R., Meyer, T.H., Bresnahan, P.A., 2004. Northeast United States and southeast Canada natural mercury emissions estimated with a surface emission model. Atmospheric Environment 38, 5683–5692.

Bauer, D., D'Ottone, L., Campuzano-Jost, P., Hynes, A.J., 2003. Gas phase elemental mercury: a comparison of LIF techniques and study of the kinetics of reaction with the hydroxyl radical. Journal of Photochemisry and Photobiology A 157, 247–256.

Bergan, T., Rodhe, H., 2001. Oxidation of elemental mercury in the atmosphere; constraints imposed by global scale modeling. Journal of Atmospheric Chemistry 40, 191–212.

Biazar, A.P., McNider, R.T., Roselle, S.J., Suggs, R.J., 2005. Correction CMAQ photolysis rate based on GOES observed clouds. In: Proceedings of the 85th American Meteorological Society Annual Meeting, San Diego.

Brezonik, P.L., 1994. Chemical Kinetics and Process Dynamics in Aquatic Systems. Lewis Publications–CRC Press, Boca Raton, FL.

Budinova, T., Savova, D., Petrov, N., Razvigorova, M., Minkova, V., Ciliz, N., Apak, E., Ekinci, E., 2003. Mercury adsorption by different modifications of furfural adsorbent. Industrial & Engineering Chemistry Research 42, 2223–2229.

Bullock, O.R., 2000. Modeling assessment of transport and deposition patterns of anthropogenic mercury air emissions in the United States and Canada. Science of the Total Environment 259, 145–157.

Bullock, O.R., Brehme, K.A., 2002. Atmospheric mercury simulation using the CMAQ model: formulation description and analysis of wet deposition results. Atmospheric Environment 36, 2135–2146.

Calvert, J.G., Lindberg, S.E., 2003. A modeling study of the mechanism of the halogen–ozone–mercury homogeneous reactions in the troposphere during the polar spring. Atmospheric Environment 37, 4467–4481.

Calvert, J.G., Lindberg, S.E., 2004. The potential influence of iodine-containing compounds on the chemistry of the

troposphere in the polar spring II: mercury depletion. Atmospheric Environment 38, 5105–5116.

Calvert, J.G., Lindberg, S.E., 2005. Mechanisms of mercury removal by O_3 and OH in the atmosphere. Atmospheric Environment 39, 3355–3367.

Clarkson, T.W., 1995. The toxicity of mercury and its compounds. In: Watras, C.J., Huckabee, J.W. (Eds.), Mercury Pollution: Integration and Synthesis, pp. 631–641.

Du, S.H., Fang, S.C., 1982. Uptake of elemental mercury vapor by C3 and C4 species. Environmental and Experimental Botany 22, 437–443.

Donohoue, D.L., Bauer, D., Hynes, A.J., 2005. Temperature and pressure dependent rate coefficients for the reaction of Hg with Cl and the reaction of Cl with Cl: a pulsed laser photolysis-pulsed laser induced fluorescence study. Physical Chemistry A 109 (34), 7732–7741.

Ebinghaus, R., Kock, H.H., Temme, C.H., Einax, J.W., Löwe, A.G., Richter, A., Burrows, J.P., Schroeder, W.H., 2002. Antarctic spring time depletion of atmospheric mercury. Environmental Science & Technology 36, 1238–1244.

Erel, Y., Pehkonen, S.O., Hoffmann, M.R., 1993. Redox chemistry of iron in fog and stratus clouds. Journal of Geophysical Research—Atmospheres 98, 18423–18434.

Fitzgerald, W.F., Engstrom, D.R., Mason, R.P., Nater, E.A., 1998. The case for atmospheric contamination in remote areas. Environmental Science & Technology 32, 1–7.

Fitzgerald, W.F., Engstrom, D.R., Lamborg, C.H., Tseng, C.M., Balcom, P.H., Hammerschmidt, C.R., 2005. Modern and historic atmospheric mercury fluxes in northern Alaska: global sources and Arctic depletion. Environmental Science & Technology 39, 557–568.

Gardfeldt, K., Jonsson, M., 2003. Is bimolecular reduction of Hg(II) complexes possible in aqueous systems of environmental importance. The Journal of Physical Chemistry A 107, 4478–4482.

Gardfeldt, K., Sommar, J., Strömberg, D., Feng, X., 2001. Oxidation of atomic mercury by hydroxyl radicals and photoinduced decomposition of methylmercury in the aqueous phase. Atmospheric Environment 35, 3039–3047.

Goodsite, M.E., Plane, J.M.C., Skov, H., 2004. A theoretical study of the oxidation of Hg^0 to $HgBr_2$ in the troposphere. Environmental Science & Technology 38, 1772–1776.

Hall, B., 1995. The gas phase oxidation of elemental mercury by ozone. Water, Air and Soil Pollution 80, 301–315.

Hedgecock, I.M., Pirrone, N., 2004. Chasing quicksilver: modeling the atmospheric lifetime of $Hg^0_{(g)}$ in the marine boundary layer at various latitudes. Environmental Science & Technology 38, 69–76.

Hedgecock, I.M., Pirrone, N., Sprovieri, F., Pesenti, E., 2003. Reactive gaseous mercury in the marine boundary layer: modeling and experimental evidence of its formation in the Mediterranean region. Atmospheric Environment 37, S41–S49.

Hicks, B.B., Meyers, T.P., 1988. Measuring and modeling dry deposition in mountainous areas. In: Unsworth, M.H., Fowler, D. (Eds.), Acid Deposition at High Elevation Sites. Kluwer Academic Publishers, Dordrecht, pp. 541–552.

Hylander, L.D., Meili, M., 2003. 500 years of mercury production: global annual inventory by region until 2000 and associated emissions. Science of the Total Environment 304 (1–3), 13–27.

Jaffe, D.A., Prestbo, E., Swartzendruber, P., Weiss-Penzias, P., Kato, S., Takami, A., Hatakeyama, S., Kajii, Y., 2005. Export of atmospheric mercury from Asia. Atmospheric Environment 39, 3029–3038.

Karabulut, S., Karabakan, A., Denizili, A., Yürüm, Y., 2001. Cadmium(II) and mercury(II) removal from aquatic solutions with low-rank Turkish coal. Separation Science and Technology 36 (16), 3657–3671.

Keeler, G.J., Gratz, L.E., Al-Wali, K., 2005. Long-term atmospheric mercury wet deposition at Underhill, Vermont. Ecotoxicology 14, 71–83.

Knipping, E.M., Dabdub, D., 2002. Modeling Cl_2 formation from aqueous NaCl particles: evidence for interfacial reactions and importance of Cl_2 decomposition in alkaline solution. Journal of Geophysical Research 107 (D18), 4360.

Laurier, F.J.G., Mason, R.P., Whalin, L., Kato, S., 2003. Reactive gaseous mercury formation in the North Pacific Ocean's marine boundary layer: a potential role of halogen chemistry. Journal of Geophysical Research—Atmospheres 108 (D17), 4529.

Lee, D.S., Nemitz, E., Fowler, D., Kingdon, R.D., 2001. Modelling atmospheric mercury transport and deposition across Europe and the UK. Atmospheric Environment 35, 5455–5466.

Lin, C.J., Pehkonen, S.O., 1997. Aqueous free radical chemistry of mercury in the presence of iron oxides and ambient aerosols. Atmospheric Environment 31, 4125–4137.

Lin, C.J., Pehkonen, S.O., 1998a. Oxidation of elemental mercury by aqueous chlorine—implications for tropospheric mercury chemistry. Journal of Geophysical Research 103, 28093–28102.

Lin, C.J., Pehkonen, S.O., 1998b. Two-phase model of mercury chemistry in the atmosphere. Atmospheric Environment 32, 2543–2558.

Lin, C.J., Pehkonen, S.O., 1999. The chemistry of atmospheric mercury: a review. Atmospheric Environment 33, 2067–2079.

Lin, X., Tao, Y., 2003. A numerical modelling study on regional mercury budget for eastern North America. Atmospheric Chemistry and Physics 3, 535–548.

Lin, C.J., Pongprueksa, P., Ho, T.C., Jang, C., 2004. Development of mercury modeling schemes within CMAQ framework: science and model implementation issues. In: Proceedings of the 2004 CMAS Models-3 Conference, Research Triangle Park, NC, October 18–20 (CD-ROM).

Lin, C.J., Lindberg, S.E., Ho, T.C., Jang, C., 2005. Development of a processor in BEIS3 for estimating vegetative mercury emission in the continental United States. Atmospheric Environment 39, 7529–7540.

Lindberg, S.E., Stratton, W.J., 1998. Atmospheric mercury speciation: concentration and behavior of reactive gaseous mercury in ambient air. Environmental Science & Technology 32, 49–57.

Lindberg, S.E., Meyers, T.P., Taylor, G.E., Turner, R.R., Schroeder, W.H., 1992. Atmosphere-surface exchange of mercury in a forest: results of modeling and gradient approaches. Journal of Geophysical Research 97 (D2), 2519–2528.

Lindberg, S.E., Hanson, P.J., Meyers, T.P., Kim, K.H., 1998. Air/surface exchange of mercury vapor over forests—the need for a reassessment of continental biogenic emissions. Atmospheric Environment 32 (5), 895–908.

Lindberg, S.E., Brooks, S., Lin, C.J., Scott, K.J., Goodsite, M., Stevens, R., Landis, M., 2002a. The dynamic oxidation of

gaseous mercury in the Arctic atmosphere at polar sunrise. Environmental Science & Technology 36, 1245–1256.

Lindberg, S.E., Dong, W., Meyers, T., 2002b. Transpiration of gaseous elemental mercury through vegetation in a subtropical wetland in Florida. Atmospheric Environment 36, 5207–5219.

Lindberg, S.E., Dong, W.J., Chanton, J., Qualls, R.G., Meyers, T., 2005. A mechanism for bimodal emission of gaseous mercury from aquatic macrophytes. Atmospheric Environment 39, 1289–1301.

Lindberg, S.E., Southworth, G., Peterson, M., Hintelmann, H., Graydon, J., St. Louis, V., Amyot, M., Krabbenhoft, D., 2003. Quantifying reemission of mercury from terrestrial and aquatic systems using stable isotopes: results from the experimental lakes area METAALICUS study. American Geophysical Union, Fall Meeting 2003. Abstract #B31E–0364.

Lindqvist, O., Rodhe, H., 1985. Atmospheric mercury—a review. Tellus 27B, 136–159.

Lu, J.Y., Schroeder, W.H., Keeler, G., 2003. Field intercomparison studies for evaluation and validation of the AESmini-SamplR (TM) technique for sampling and analysis of total particulate mercury in the atmosphere. Science of the Total Environment 304, 115–125.

Manohar, D.M., Krishnan, K.A., Anirudhan, T.S., 2002. Removal of mercury(II) from aqueous solutions and chloralkali industry wastewater using 2-mercaptobenzimidazole-clay. Water Research 36, 1609–1619.

Mason, R.P., Sheu, G.R., 2002. Role of the ocean in the global mercury cycle. Global Biogeochemical Cycles 16 (4), 1093.

Miller, E.K., Vanarsdale, A., Keeler, G.J., Chalmers, A., Poissant, L., Kamman, N.C., Brulotte, R., 2005. Estimation and mapping of wet and dry mercury deposition across northeastern North America. Ecotoxicology 14, 53–70.

Munthe, J., 1992. The aqueous oxidation of elemental mercury by ozone. Atmospheric Environment 26A, 1461–1468.

Munthe, J., Xiao, Z.F., Lindqvist, O., 1991. The aqueous reduction of divalent mercury by sulfite. Water, Air and Soil Pollution 56, 621–630.

Pacyna, E.G., Pacyna, J.M., Pirrone, N., 2001. European emissions of atmospheric mercury from anthropogenic sources in 1995. Atmospheric Environment 35 (17), 2987–2996.

Pacyna, J.M., Pacyna, E.G., Steenhuisen, F., Wilson, S., 2003. Mapping 1995 global anthropogenic emissions of mercury. Atmospheric Environment 37 (S1), 109–117.

Pai, P., Karamchandani, P., Seigneur, C., 1997. Simulation of the regional atmospheric transport and fate of mercury using a comprehensive Eulerian model. Atmospheric Environment 31, 2717–2732.

Pai, P., Karamchandani, P., Seigneur, C., 2000. On artificial dilution of point source mercury emissions in a regional atmospheric model. Science of the Total Environment 259, 159–168.

Pai, P., Karamchandani, P., Seigneur, C., Allan, M.A., 1999. Sensitivity of simulated atmospheric mercury concentrations and deposition to model input parameters. Journal of Geophysical Research—Atmospheres 104, 13855–13868.

Pal, B., Ariya, P.A., 2003. Atmospheric reactions of gaseous mercury with ozone and hydroxyl radical: kinetics and product studies. Journal de Physique IV 107, 189–192.

Pal, B., Ariya, P.A., 2004a. Studies of ozone initiated reactions of gaseous mercury: kinetics, product studies and atmospheric implications. Physical Chemistry Chemical Physics 6 (3), 572–579.

Pal, B., Ariya, P.A., 2004b. Gas-phase HO-initiated reaction of elemental mercury: kinetics, product studies, and atmospheric implications. Environmental Science & Technology 38, 5555–5566.

Pehkonen, S.O., Lin, C.-J., 1998. Aqueous photochemistry of divalent mercury with organic acids. Journal of the Air & Waste Management Association 48, 144–150.

Petersen, G., Iverfeldt, A., Munthe, J., 1995. Atmospheric mercury species over central and northern Europe: model calculations and comparison with measurements from the Nordic air and precipitation network for 1987 and 1988. Atmospheric Environment 29, 47–67.

Poissant, L., Pilote, M., Xu, X., Zhang, H., Beauvais, C., 2004. Atmospheric mercury speciation and deposition in the Bay St. François wetlands. Journal of Geophysical Research 109, D11301.

Porcella, D.B., Ramel, C., Jernelöv, A., 1997. Global mercury pollution and the role of gold mining: an overview. Water, Air and Soil Pollution 97, 205–207.

P'yankov, V.A., 1949. Kinetics of the reaction between mercury vapor and ozone. Zhurnal Obshchei Khimii (Journal of General Chemistry) 19, 187–192.

Raofie, F., Ariya, P.A., 2003. Kinetics and products study of the reaction of BrO radicals with gaseous mercury. Journal de Physique IV 107, 1119–1121.

Raofie, F., Ariya, P.A., 2004. Product study of the gas-phase BrO-initiated oxidation of Hg-0: evidence for stable Hg^{1+} compounds. Environmental Science & Technology 38, 4319–4326.

Ryaboshapko, A., Bullock, R., Ebinghaus, R., Ilyin, I., Lohman, K., Munthe, J., Petersen, G., Seigneur, C., Wangberg, I., 2002. Comparison of mercury chemistry models. Atmospheric Environment 36, 3881–3898.

Ryaboshapko, A., Artz, R., Bullock, R., Christensen J., Cohen, M., Drexler, R., Ilyin, I., Munthe, J., Pacyna, J., Petersen, G., Syrakov, D., Tranikov, O., 2005. Intercomparison study of numerical models for long-range atmospheric transport of mercury. EMEP/MSC-E Technical Report, Leningradsky, 16/2, 125040 Moscow, Russia.

Sanchez-Polo, M., Rivera-Utrilla, J., 2002. Adsorbent–adsorbate interactions in the adsorption of Cd(II) and Hg(II) on ozonized activated carbons. Environmental Science & Technology 36, 3850–3854.

Schell, D., Wobrock, W., Maser, R., Preiss, M., Jaeschke, W., Georgii, H.W., Gallagher, M.W., Beswick, K.M., Pahl, S., Facchini, M.C., Fuzzi, S., Wiedensohler, A., Hansson, H.C., Wendisch, M., 1997. The size-dependent chemical composition of cloud droplets. Atmospheric Environment 31 (16), 2561–2576.

Schroeder, W.H., Munthe, J., 1998. Atmospheric mercury: an overview. Atmospheric Environment 32, 809–822.

Schroeder, W.H., Yardwood, G., Nikki, H., 1991. Transformation process involving Hg species in the atmosphere—results for a literature survey. Water, Air and Soil Pollution 56, 652–666.

Schroeder, W.H., Analuf, K.G., Barrie, L.A., Lu, J.Y., Steffen, A., Schneeberger, D.R., Berg, T., 1998. Artic springtime depletion of mercury. Nature 394, 331–332.

Seigneur, C., Abeck, H., Chia, G., Reinhard, M., Bloom, N.S., Prestbo, E., Saxena, P., 1998. Mercury adsorption to elemental carbon (soot) particles and atmospheric particulate matter. Atmospheric Environment 32, 2649–2657.

Seigneur, C., Lohman, K., Pai, P., Heim, K., Mitchell, D., Levin, L., 1999. Uncertainty analysis of regional mercury exposure. Water, Air and Soil Pollution 112, 151–162.

Seigneur, C., Karamchandani, P., Lohman, K., Vijayaraghavan, K., Shia, R.L., 2001. Multiscale modeling of the atmospheric fate and transport of mercury. Journal of Geophysical Research—Atmospheres 106, 27795–27809.

Seigneur, C., Karamchandani, P., Vijayaraghavan, K., Lohman, K., Shia, R.L., Levin, L., 2003a. On the effect of spatial resolution on atmospheric mercury modeling. Science of the Total Environment 304, 73–81.

Seigneur, C., Lohman, K., Vijayaraghavan, K., Shia, R.L., 2003b. Contributions of global and regional sources to mercury deposition in New York State. Environmental Pollution 123, 365–373.

Seigneur, C., Vijayaraghavan, K., Lohman, K., Karamchandani, P., Scott, C., Levin, L., 2003c. Simulation of the fate and transport of mercury in North America. Journal de Physique IV 107, 1209–1212.

Seigneur, C., Vijayaraghavan, K., Lohman, K., Karamchandani, P., Scott, C., 2004. Global source attribution for mercury deposition in the United States. Environmental Science & Technology 38, 555–569.

Senior, C.L., Johnson, S.A., 2005. Impact of carbon-in-ash on mercury removal across particulate control devices in coal-fired power plants. Energy & Fuels 19 (3), 859–863.

Seinfeld, J.H., Pandis, S.N., 1997. Atmospheric Chemistry and Physics. Wiley-Interscience, New York, pp. 350–351.

Senior, C.L., Helble, J.J., Sarofim, A.F., 2000. Emissions of mercury, trace elements, and fine particles from stationary combustion sources. Fuel Processing Technology 65, 263–288.

Shia, R.L., Seigneur, C., Pai, P., Ko, M., Sze, N.D., 1999. Global simulation of atmospheric mercury concentrations and deposition fluxes. Journal of Geophysical Research—Atmospheres 104, 23747–23760.

Skov, H., Christensen, J.H., Goodsite, M.E., Heidam, N.Z., Jensen, B., Wahlin, P., Geernaert, G., 2004. Fate of elemental mercury in the artic during atmospheric mercury depletion episodes and the load of atmospheric mercury to the artic. Environmental Science & Technology 38, 2373–2382.

Slemr, F., Brunke, E.G., Ebinghaus, R., Temme, C., Munthe, J., Wängberg, I., Schroeder, W., Steffen, A., Berg, T., 2003. Worldwide trend of atmospheric mercury since 1977. Geophysical Research Letters 30 (10), 1516.

Smith, R.M., Martell, A.E., 2004. NIST Critically Selected Stability Constants of Metal Complexes Database Version 8. National Institute of Standards and Technology, Gaithersburg, MD 20899.

Sommar, J., Gårdfeldt, K., Strömberg, D., Feng, X., 2001. A kinetic study of the gas-phase reaction between the hydroxyl radical and atomic mercury. Atmospheric Environment 35, 3049–3054.

Streets, D.G., Haob, J., Wu, Y., Jiang, J., Chan, M., Tian, H., Feng, X., 2005. Anthropogenic mercury emissions in China. Atmospheric Environment 39, 7789–7806.

Stumm, W., Morgan, J.J., 1995. Aquatic Chemistry: Chemical Equilibria and Rates in Natural Waters, third ed. Wiley-Interscience, New York.

Taylor, G., 1913. The dissociation of mercuric oxide. Journal of Physical Chemistry 17, 565–591.

Tokos, J.J.S., Hall, B., Calhoun, J.A., Prestbo, E.M., 1998. Homogeneous gas-phase reaction of Hg^0 with H_2O_2, O_3, CH_3I, and $(CH_3)_2S$: implications for atmospheric Hg cycling. Atmospheric Environment 32, 823–827.

United States Environmental Protection Agency (USEPA), 1997. Mercury Study Report to Congress, EPA-452/R-97-003, Office of Air Quality Planning and Standards, Office of Research and Development, US Government Printing Office, Washington, DC.

Van Loon, L., Mader, E., Scott, S.L., 2000. Reduction of the aqueous mercuric ion by sulfite: UV spectrum of $HgSO_3$ and its intramolecular redox reaction. The Journal of Physical Chemistry A 104, 1621–1626.

Vanarsdale, A., Weiss, J., Keeler, G., Miller, E., Boulet, G., Brulotte, R., Poissant, L., 2005. Patterns of mercury deposition and concentration in northeastern North America (1996–2002). Ecotoxicology 14, 37–52.

Vogt, R., Crutzen, P.J., Sander, R., 1996. A mechanism for halogen release from sea-salt aerosol in the remote marine boundary layer. Nature 382, 327–330.

Von Glasow, R., Sander, R., Bott, A., Crutzen, P.J., 2002a. Modeling halogen chemistry in the marine boundary layer 1. Cloud-free MBL. Journal of Geophysical Research 107 (D17), 4341.

Von Glasow, R., Sander, R., Bott, A., Crutzen, P.J., 2002b. Modeling halogen chemistry in the marine boundary layer 2. Interactions with sulfur and the cloud-covered MBL. Journal of Geophysical Research 107 (D17), 4323.

Walcek, C., De Santis, S., Gentile, T., 2003. Preparation of mercury emissions inventory for eastern North America. Environmental Pollution 123, 375–381.

Wang, Z., Pehkonen, S.O., 2004. Oxidation of elemental mercury by aqueous bromine: atmospheric implications. Atmospheric Environment 38, 3675–3688.

Wesely, M.L., 1989. Parameterization of surface resistances to gaseous dry deposition in regional-scale numerical models. Atmospheric Environment 23, 1293–1304.

Xiao, B., Thomas, K.M., 2004. Competitive adsorption of aqueous metal ions on an oxidized nanoporous activated carbon. Langmuir 20, 4566–4578.

Xiao, Z.F., Munthe, J., Stromberg, D., Lindqvist, O., 1994. Photochemical behavior of inorganic mercury compounds in aqueous solution. In: Watras, C.J., Huckabee, J.W. (Eds.), Mercury as a Global Pollutant—Integration and Synthesis. Lewis Publishers, pp. 581–592.

Xu, Y., Carmichael, G.R., 1998. Modeling the dry deposition velocity of sulfur dioxide and sulfate in Asia. Journal of Applied Meteorology 37, 1084–1099.

Xu, X., Yang, X., Miller, D.R., Helble, J.J., Carley, R.J., 1999. Formulation of bi-directional atmosphere-surface exchanges of elemental mercury. Atmospheric Environment 33, 4345–4355.

Xu, X., Yang, X., Miller, D.R., Helble, J.J., Carley, R.J., 2000. A regional scale modeling study of atmospheric transport and transformation of mercury. I. Model development and evaluation. Atmospheric Environment 34, 4933–4944.

Yin, Y., Allen, H.E., Huang, C.P., Sanders, P.F., 1997. Adsorption/desorption isotherms of Hg(II) by soil. Soil Science 162 (1), 35–45.